PHYSICAL REVIEW B **94**, 155133 (2016)

Heterodyne Hall effect in a two-dimensional electron gas

Takashi Oka and Leda Bucciantini
Max Planck Institute for the Physics of Complex Systems, Nöthnitzer Strasse 38, D-01187 Dresden, Germany and Max Planck Institute for Chemical Physics of Solids, Nöthnitzer Strasse 40, D-01187 Dresden, Germany
(Received 11 July 2016; published 20 October 2016)

We study the hitherto unaddressed phenomenon of the quantum Hall effect with a magnetic and electric field oscillating in time with resonant frequencies. This phenomenon highlights an example of a heterodyne device with the magnetic field acting as a driving force, and it is analyzed in detail in its classical and quantum versions using Floquet theory. A bulk current flowing perpendicularly to the applied electric field is found, with a frequency shifted by integer multiples of the driving frequency. When the ratio of the cyclotron and driving frequency takes special values, the electron's classical trajectory forms a loop and the effective mass diverges, while in the quantum case we find an analog of the Landau quantization. A possible realization using metamaterial plasmonics is discussed.

DOI: 10.1103/PhysRevB.94.155133

I. INTRODUCTION

The quantum Hall effect (QHE) is one of the most complex phenomena in condensed-matter physics. When a static electric field is applied to a quantum Hall state, a current perpendicular to the field is induced, and their linear relation $j_x = \sigma^H E_y$ is given by the Hall conductivity $\sigma^H = \frac{e^2}{h}\nu$ [1]. In the integer quantum Hall effect (IQHE), the factor ν is strictly an integer, and it was related to a topological index, the first Chern number, by Thouless, Kohmoto, Nightingale, and den Nijs [2]. The process is dissipationless because the current is perpendicular to the field and no Joule heating takes place.

Here, we report an extension of this concept to the physically interesting case when the magnetic and electric fields are time-dependent with resonant frequencies. This highlights an example of a heterodyne response, which is a ubiquitous technique in today's electronics with various usages, such as high-precision optical detection [3–5]. A heterodyne (frequency mixer) is an electronic device that mixes frequencies of oscillating signals through a nonlinear process [Fig. 1(a)]. It is periodically driven by a "local oscillator" with frequency Ω, and integer multiples of Ω are added or subtracted to the frequency ω of the input signal. Here we will be interested in studying a heterodyne system in which the driving oscillator is the magnetic field while the input signal is an electric field [Fig. 1(b)].

An important example of periodically driven systems is the zero resistance state that occurs in a two-dimensional electron gas (2DEG) driven by microwaves in a semiconductor heterostructure in weak magnetic fields [6] (reviewed in Ref. [7]). More recently, periodically driven lattice systems have been attracting interest [8–11] as a way to realize a topological Chern insulator [12], which was recently confirmed experimentally [13,14]. However, we stress that these examples focused on the response of the system to a static electric field, and the heterodyne response has not yet been the subject of a detailed investigation. In this paper, we set out to fill this gap and develop a theory for the heterodyne response by studying the conductivity of a 2DEG confined in the xy plane subject to a z-directed magnetic field,

$$B_z(t) = B\cos\Omega t, \qquad (1)$$

with an oscillating electric field [see Fig. 1(b)]. We will focus on the strong nonlinear effects introduced when the frequencies of the driving and of the electric field are resonant, i.e., when $\omega = n\Omega$, $n \in \mathbb{N}$.

The paper is organized as follows. In Secs. II and III we develop a theory for this system at the classical and quantum level, respectively, while in Sec. IV we summarize our results and discuss open problems.

II. CLASSICAL CASE

In this section, we study the response of a classical 2DEG to a time-oscillating weak electric field in the presence of an oscillating magnetic field, and we compute the conductivity tensor, which we call heterodyne conductivity. The heterodyne conductivity $\sigma_{ab}^{m,n}$, introduced here for both classical and quantum cases, is a four-index tensor implicitly defined by the linear relation that holds between the electric current density $j_a(m\Omega)$ of the output signal with frequency $m\Omega$, flowing along the a direction $(a,b = x,y,z)$ and the (weak) electric field E_b^n along the b direction with frequency $n\Omega$.

Given an electric signal $E_b(t) = E_b(\omega)e^{-i\omega t}$ along a direction b with frequency ω, the output current generated from the heterodyne along a direction a can be expanded in modes with frequencies $\omega + l\Omega$, with l a generic integer, as $j_a(t) = \sum_l j_a(\omega + l\Omega)e^{-i(\omega+l\Omega)t}$. Then the linear relation

$$j_a(\omega + l\Omega) = \sum_b \tilde{\sigma}_{ab}^l(\omega)E_b(\omega) \qquad (2)$$

holds as long as the field is weak and defines the conductivity $\tilde{\sigma}_{ab}^l(\omega)$. When $\omega = n\Omega$, with $n \in \mathbb{N}$, defining $E_b(n\Omega) \equiv E_b^n$ and $l + n = m$, (2) can be rewritten as

$$j_a(m\Omega) = \sum_b \tilde{\sigma}_{ab}^{m-n}(n\Omega)E_b^n. \qquad (3)$$

Defining $\tilde{\sigma}_{ab}^{m-n}(n\Omega) \equiv \sigma_{ab}^{m,n}$, so that the upper left index labels the component of the outgoing current while the upper right index labels the component of input electric field, Eq. (3) gives

$$j_a(m\Omega) = \sum_b \sum_{n=-\infty}^{\infty} \sigma_{ab}^{m,n} E_b^n. \qquad (4)$$

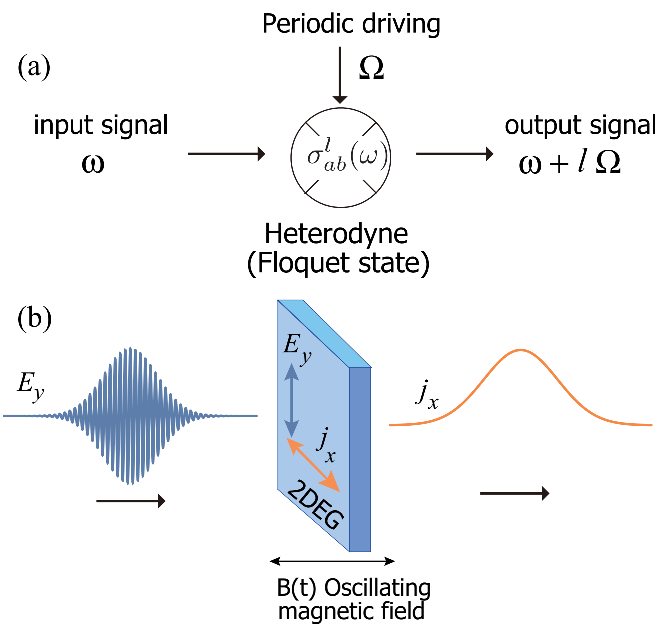

FIG. 1. (a) A heterodyne mixes the frequency ω of the input signal with its driving frequency Ω. The output is a superposition of signals with frequencies $\omega + l\Omega$, $l \in \mathbb{Z}$. (b) Model under study: an input electric field directed along y and a magnetic field oscillating in time along z, acting on a two-dimensional electron gas (2DEG): this yields an electric current along x, with a frequency different from that of the input electric field. In this example, the input is a single mode with an envelope function, and the output is the zero-frequency envelope, which are related by the coefficient $\sigma_{xy}^{-1}(\Omega)$.

More explicitly, the heterodyne conductivity $\sigma_{ab}^{m,n}$ is obtained inverse Fourier transforming (4),

$$\sigma_{ab}^{m,n} = \lim_{t_0\to\infty} \frac{1}{t_0 E_b^n} \int_0^{t_0} dt\, e^{im\Omega t} j_a(t) \tag{5}$$

with $j_a(t) = en_e v_a(t)$.

The current density $j_a(t)$ is related to the electron's velocity $v_a(t)$ by the relation $j_a(t) = n_e e v_a(t)$, with $e < 0$ the electron's charge and n_e the electron's density; the velocity $v_a(t)$ can be derived from the solution of the classical equation of motion

$$m_e\left(\frac{d}{dt} + \eta\right)\boldsymbol{v}(t) = e\left(\boldsymbol{E} + \frac{1}{c}\boldsymbol{v}(t) \times \boldsymbol{B}(t)\right), \tag{6}$$

where m_e is the electron's mass while η is a small phenomenological scattering parameter necessary for the convergence of the particle's trajectory in electric fields; $\boldsymbol{B}(t) = B_z(t)\hat{\mathbf{z}}$ is the oscillating magnetic field (1), and $\boldsymbol{E}$ is the (infinitesimal) applied electric field. We note that we have neglected the electric field emerging from the time-dependent magnetic field, which will be recovered in the quantum case. Given the rotational invariance of the system, we arbitrarily fix the direction of the electric field as the y direction and restrict our analysis to $\{n,m\} = 0,1$, with $E_y(t) = E_y^0$ $(n = 0)$ and $E_y(t) = E_y^1 \cos(\Omega t)$ $(n = 1)$. The behavior of the particle strongly depends on the ratio

$$r = \frac{\omega_c}{\Omega}, \tag{7}$$

with $\omega_c = |e|B/m_e c$ the cyclotron frequency.

The formulas for the heterodyne conductivities can be derived as follows. Defining

$$v(t) = v_x(t) + i v_y(t), \tag{8}$$

the equation of motion (6) for $\mathbf{E} = E_y^0\hat{\mathbf{y}}$ becomes

$$\dot{v}(t) = i\frac{eE_y^0}{m_e} + v(t)\left(-i\frac{eB_z(t)}{m_e c} - \eta\right), \tag{9}$$

whose solution is

$$v(t) = i\frac{eE_y^0}{m_e} e^{-\eta t + ir\sin(\Omega t)} \int_0^t ds\, e^{\eta s - ir\sin(\Omega s)}. \tag{10}$$

The results for the conductivities are thus

$$\sigma_{xy}^{0,0} + i\sigma_{yy}^{0,0} = i\frac{e^2 n_e}{m_e} \sum_{n=-\infty}^{\infty} \frac{J_n(r)^2}{\eta - i\Omega n},$$

$$\sigma_{xy}^{1,0} + i\sigma_{yy}^{1,0} = i\frac{e^2 n_e}{m_e} \sum_{n=-\infty}^{\infty} \frac{J_n(r)J_{1-n}(r)(-1)^n}{\eta + i\Omega(1-n)},$$

where $J_n(r)$ is the nth Bessel function of the first kind. From the former of these equations, we derive

$$\sigma_{xy}^{0,0} = 0, \quad \sigma_{yy}^{0,0} = \frac{e^2 n_e}{m_e \eta} J_0(r)^2. \tag{11}$$

When applying an oscillating electric field along the y direction with $\mathbf{E}(t) = E_y^1 \cos(\Omega t)\hat{\mathbf{y}}$, the solution for $v(t)$ is

$$v(t) = i\frac{eE_y^1}{m_e} e^{-\eta t + ir\sin(\Omega t)} \int_0^t ds\, e^{\eta s - ir\sin(\Omega s)} \cos(\Omega s),$$

and, as a result, we get

$$\sigma_{xy}^{0,1} + i\sigma_{yy}^{0,1} = i\frac{e^2 n_e}{m_e} \sum_{n=-\infty}^{\infty} \frac{J_n(x)J_{n-1}(x)}{\eta + i\Omega n}. \tag{12}$$

Figure 2(a) shows the results for the static diagonal and transverse conductivity (all in absolute values) $\sigma_{yy}^{0,0}, \sigma_{xy}^{0,0}$ and the inverse heterodyne Hall conductivity $1/\sigma_{xy}^{1,0}$, $1/\sigma_{xy}^{0,1}$ as a function of r. The diagonal conductivity $\sigma_{yy}^{0,0}$ first decreases when enlarging B and vanishes at a discrete set of points, labeled as $r = r_\alpha^{\text{cl}}$ $(\alpha = 1,2,3,\ldots)$.

This behavior can be understood from the dynamics of the particles in zero electric field [Fig. 2(b)], which is no longer the cyclotron motion in an oscillating magnetic field. In static but spatially inhomogeneous fields, particles make detours and their paths were called "snake states" [15]. This generally also takes place in temporary oscillating magnetic fields [16], and the detour makes the particles "heavy." We can relate the diagonal conductivity with the particle's effective mass m_{cl}^* by $m_e/m_{\text{cl}}^* = \sigma_{yy}^{0,0}/\sigma_0$, with $\sigma_0 = e^2 n_e/(\eta m_e)$ being the zero-field expression [17]. When the diagonal conductivity $\sigma_{yy}^{0,0}$ vanishes at $r = r_\alpha^{\text{cl}}$, the particle's trajectory in zero external field forms closed loops, and the index α used to identify them has a topological meaning of a winding number per half-period. Indeed, to have a closed trajectory, no dissipative process should be present, which implies a vanishing diagonal conductivity. The static transverse conductivity is expected to

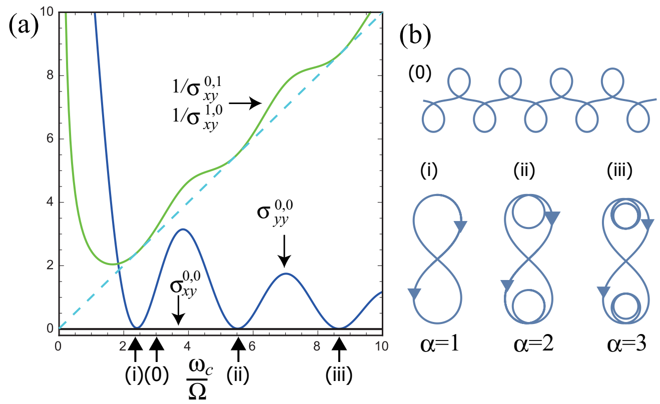

FIG. 2. (a) Static and heterodyne conductivities of a classical particle in an oscillating magnetic field. The dashed line represents the classical result for the resistivity in a static magnetic field. The parameter η is 0.05, $n_e = m_e = |e| = 1$. $r = r^{cl}_\alpha$ are identified as the zeros of the Bessel function $J_0(r)$, explicitly $r^{cl} = \{2.40, 5.52, 8.67, \ldots\}$. (b) Trajectories of the charged particle for different values of r in zero electric field. (0) For general values, the particle makes open detours. (i)–(iii) For $r^{cl}_1 = 2.40$ (i), $r^{cl}_2 = 5.52$ (ii), and $r^{cl}_3 = 8.67$ (iii), the trajectory forms a closed periodic orbit, whose winding number per half cycle $T/2 = \pi/\Omega$ is an integer $\alpha = 1,2,3$, respectively.

vanish due to time-reversal invariance of the system on time scales that are multiples of a period.

The system also shows a nontrivial heterodyne Hall response. The Hall conductivity $\sigma^{0,1}_{xy}$, which coincides with $\sigma^{1,0}_{xy}$, takes values close to the classical result $(n_e|e|c)/B$ when the field is strong enough [Fig. 2(a)]. In particular, they coincide when the effective mass diverges at $r = r^{cl}_\alpha$; we note that this feature is present also in the quantum case.

III. QUANTUM CASE

Let us now consider a quantum version of the heterodyne Hall effect in a one-particle system. This is obtained with the minimal substitution starting from free electrons ($p^\mu \to p^\mu - e/cA^\mu$, with $\mu = 1,2$); in the Landau gauge, the vector potential is $A_x(t) = 0$, $A_y(t) = B_z(t)x$, which generates the electromagnetic field

$$B_z(t) = B\cos\Omega t, \quad E_y(t) = -\frac{\partial B_z(t)}{\partial t}x. \tag{13}$$

The quantum Hamiltonian is

$$H(t) = \frac{\hbar^2 k_y^2}{2m_e} + H_0(x,t) - F(t)x, \tag{14}$$

where $H_0(x,t) = \frac{p_x^2}{2m_e} + \frac{m_e[\omega(t)]^2}{2}x^2$ is the Hamiltonian of a quantum harmonic oscillator (HO) with an oscillating frequency $\omega(t) = \omega_c\cos\Omega t$. $F(t)$ is a driving term that contains the (infinitesimal) input electric field, which we choose as $E_x(t) = E^1_x\cos\Omega t$, and it has the form $F(t) = \omega(t)\hbar k_y - eE_x(t)$. We emphasize that translational invariance in the y direction still holds.

Using the time periodicity of the Hamiltonian $H(t+T) = H(t)$ for $T = 2\pi/\Omega$, we seek a solution of the time-dependent Schrödinger equation in the Floquet form [18–21]

$$\Psi_n(\boldsymbol{x},t) = e^{-\frac{i}{\hbar}E_n(k_y)t}\Phi_n(\boldsymbol{x},t), \tag{15}$$

where $\Phi_n(\boldsymbol{x},t)$ is a periodic function in time and $E_n(k_y)$ is the Floquet quasienergy. To be more precise, because (15) is a Floquet solution, it will be labeled by a combined index $\alpha = (n,m)$, where n is the HO energy level and $m = 0, \pm 1, \pm 2, \ldots$ represents replica states ("photon-absorbed state").

Using the transformation by Taniuti and Husimi [22], the Floquet state [23] is given by

$$\Phi_n(\boldsymbol{x},t) = \frac{e^{ik_y y}}{\sqrt{L_y}}\varphi_n(x - X(t),t)\exp\left[\frac{i}{\hbar}\left\{m_e\dot{X}(t)[x - X(t)] + \int_0^t dt' L(t') - L_0 t\right\}\right]. \tag{16}$$

Here, $\varphi_n(x,t)$ is the solution of the eigenvalue problem $[H_0(x,t) - i\hbar\frac{\partial}{\partial t}]\varphi_n(x,t) = \varepsilon_n\varphi_n(x,t)$, with energy ε_n; the wave-packet center $X(t)$ is the solution of the equation of motion for a classical HO with a driving term $F(t)$: $m_e\ddot{X}(t) + m_e\omega(t)^2X(t) = F(t)$; $L(t)$ and L_0 are, respectively, the Lagrangian and its time average for this driven HO, given by $L(t) = \frac{1}{2}m_e\dot{X}^2(t) - \frac{1}{2}m_e\omega(t)^2X^2(t) + X(t)F(t)$ and $L_0 = \frac{1}{T}\int_0^T L(t')dt'$. The expression for $E_n(k_y)$ in (15) is related to ε_n by

$$E_n(k_y) = \epsilon_n - L_0 + \frac{\hbar^2 k_y^2}{2m_e}. \tag{17}$$

To extract the solution for $X(t)$, it is convenient to introduce a dimensionless variable $\xi(\tau)$,

$$X(t) = -(l_B r)^2\xi(\tau)\left(k_y - \frac{eE^1_x}{\hbar\omega_c}\right), \tag{18}$$

where $\tau = \Omega t$, $l_B = \sqrt{\hbar c/eB}$ is the magnetic length, and $\xi(\tau)$ is the solution for Mathieu's equation with a source term $\xi''(\tau) + 2a\cos^2\tau\,\xi(\tau) = -\cos\tau$, with $a = r^2/2$. The variable ξ inherits the periodicity $\xi(\tau + 2\pi) = \xi(\tau)$ from X and oscillates around $x = 0$ as shown in Fig. 3(a). This is obtained by writing $\xi(\tau) = \sum_m \xi_m e^{-im\tau}$ and solving the linear relation $\xi_m(-m^2 + \frac{r^2}{2}) + \frac{r^2}{4}(\xi_{m-2} + \xi_{m+2}) + \frac{1}{2}\delta_{m^2,1} = 0$.

To derive the Floquet spectrum ϵ_n and the wave function $\varphi_n(x,t)$, we have to compute the Floquet Hamiltonian $\mathcal{H}(x,t) = H_0(x,t) - i\hbar\frac{\partial}{\partial t}$, whose matrix elements in the Floquet basis $|m(t)\rangle = e^{-imt}$ are given, as usual, by

$$\mathcal{H}^{m,m'} = \frac{1}{T}\int dt\, e^{i(m-m')\Omega t}H_0(x,t) + m\delta_{m,m'}\Omega. \tag{19}$$

After conveniently rewriting $H_0(x,t)$ as

$$H_0(x,t) = \frac{p_x^2}{2m_e} + \frac{m_e\bar{\omega}^2}{2}x^2 + \frac{1}{4}m_e\bar{\omega}^2x^2(e^{2i\Omega t} + e^{-2i\Omega t}), \tag{20}$$

with $\bar{\omega} = \omega_c/\sqrt{2}$, (19) yields

$$\mathcal{H}^{m,m'} = \left(\frac{p_x^2}{2m_e} + \frac{m_e\bar{\omega}^2}{2}x^2 + m\hbar\Omega\right)\delta_{m,m'} + \frac{1}{4}m_e\bar{\omega}^2x^2(\delta_{m,m'+2} + \delta_{m,m'-2}). \tag{21}$$

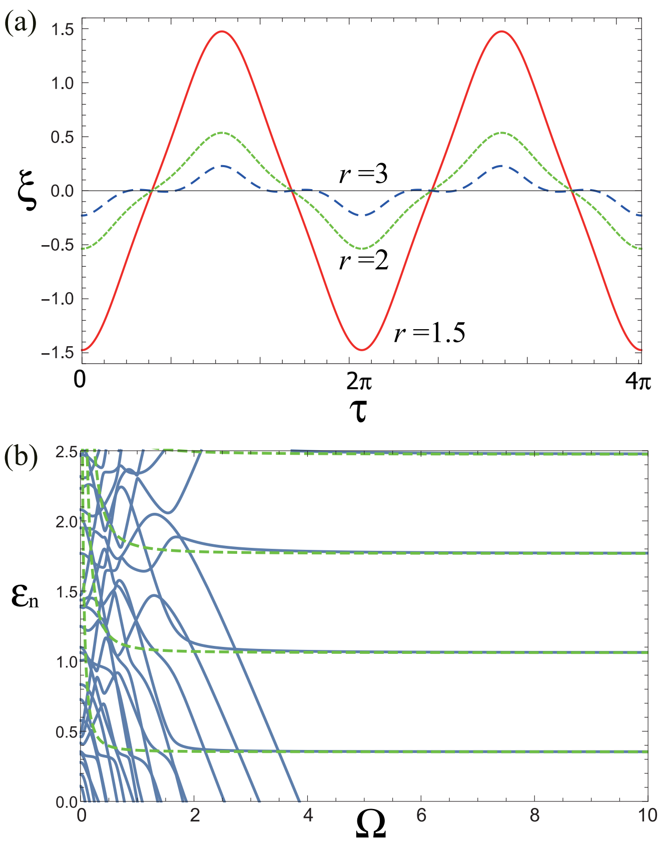

FIG. 3. (a) Plot of $\xi(\tau)$ defined in (18) for $r = 1.5,2,3$. (b) The intricate Floquet spectrum (solid lines) reduces, for large enough Ω, to equispaced energy levels of a quantum HO (dashed lines) with frequency $\omega_{\rm eff}$.

Using the Floquet-Magnus expansion [24,25] and $[[\frac{p^2}{2m},V(x)],V(x)] = -\frac{1}{m}(\frac{\partial V}{\partial x})^2$, the high-frequency effective Hamiltonian, up to order Ω^{-2}, is

$$H_{\rm eff} = H^{0,0} + \frac{[[H^{2,0},H^{00}],H^{2,0}]}{(2\Omega)^2} = \hbar\omega_{\rm eff}(\Omega)(n+1/2) \tag{22}$$

with $\omega_{\rm eff}(\Omega) = \frac{\omega_c}{\sqrt{2}}\sqrt{1+\frac{1}{16}(\frac{\omega_c}{\Omega})^2}$. Therefore, in the large Ω limit, the energy eigenvalues reduce to those of a static quantum HO with a renormalized frequency that depends on the driving Ω,

$$\epsilon_n = \hbar\omega_{\rm eff}(\Omega)(n+1/2). \tag{23}$$

In Fig. 3(b) we present the full Floquet spectrum ϵ_n as a function of Ω (solid lines), obtained by diagonalizing (21). For large Ω values, it agrees well with the high-frequency effective spectrum (23) (dashed lines). In this limit, the wave function φ_n in (16) is the usual HO eigenstate, i.e., $e^{-x^2/2l^2}H_n(x/l)$ with $l = (\hbar m_e/\omega_{\rm eff})^{1/2}$, while the orbital mixing increases as Ω becomes smaller.

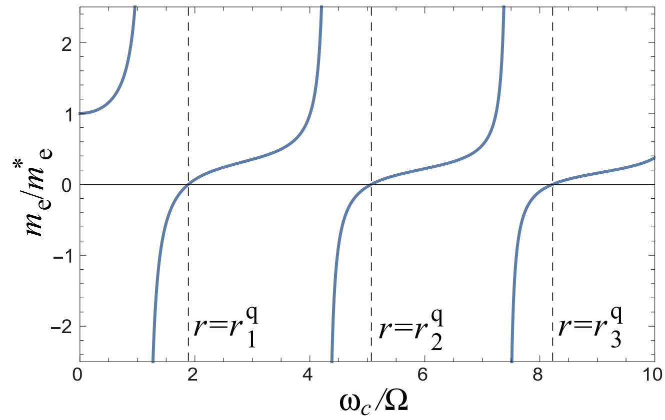

FIG. 4. The inverse effective mass $\frac{m_e}{m_e^*}$ as a function of r. The effective mass diverges at $r = r_\alpha^{\rm q}$, resulting in the Landau quantization.

The Floquet quasienergy $E_n(k_y)$ can be further calculated from (17), resulting in

$$E_n(k_y) = \epsilon_n + \frac{\hbar^2 k_y^2}{2m_e} - \frac{\hbar^2}{2m_e}\left(1-\frac{m_e}{m_e^*}\right)\left(k_y - \frac{eE_x^1}{\hbar\omega_c}\right)^2, \tag{24}$$

where the effective mass m_e^* is given by

$$\frac{m_e}{m_e^*} = 1 + \frac{r^2}{2\pi}\int_0^{2\pi} d\tau \cos\tau\,\xi(\tau) \tag{25}$$

plotted in Fig. 4. We can compare this plot with that of the classical longitudinal conductivity $\sigma_{yy}^{0,0} \sim m_e/m_{\rm cl}^*$ shown in Fig. 2(a). First, we see that the effective mass m_e^* diverges at certain ratios $r = r_\alpha^{\rm q}$ collected in Table I. When this happens, the k_y dependence in (24) drops out in the absence of E_x^1 and a macroscopic number of states become degenerate, an analog of Landau quantization now realized by the oscillating magnetic/electric fields (13). Around $r = r_\alpha^{\rm q}$, the effective mass changes sign from negative (holelike) to positive (electronlike). Mathematically, the condition for divergent ($r = r_\alpha^{\rm q}$) and zero effective mass, i.e., $|m_e^*| \to \infty,0$, coincides with the periodic solution condition of the Mathieu equation without the source term.

The quantum version of the heterodyne Hall effect occurs when we turn on the x direction ac electric field E_x^1 leading to a dc current flowing in the y direction. We can compute the dc current $J_y(k_y) = e\frac{\partial E_n}{\hbar\partial k_y}$ for a state with k_y as the momentum derivative of the dispersion relation (24) as in the static case. The total current density for a system of dimensions $L_x \times L_y$ is defined as $j_y = \frac{1}{L_xL_y}\sum_{k_y} f_n(k_y)J_y(k_y)$, and given that the distribution $f_n(k_y)$ is even in k_y due to the invariance under

TABLE I. The values for the constant Q are reported for the first four $r = r_\alpha^{\rm q}$.

α	1	2	3	4
$r_\alpha^{\rm q}$	1.89	5.07	8.22	11.37
Q	0.221	0.153	0.124	0.106

time reversal, we obtain a linear relation

$$j_y = \sigma_{yx}^{0,1} E_x^1, \tag{26}$$

where the heterodyne Hall coefficient is given by

$$\sigma_{yx}^{0,1} = \frac{e^2}{h} Q\nu. \tag{27}$$

The Landau level filling $\nu = N_e/N_\Phi$ is defined as the ratio of the electron density N_e and the level degeneracy

$$N_\Phi = \frac{L_x L_y}{2\pi l_B^2 r^2 \max \xi}; \tag{28}$$

N_Φ is obtained by imposing the wave-packet center (18) to be within the strip, i.e., $X(t) \in [-L_x/2, L_x/2]$ for $E_x^1 = 0$, where max ξ is the maximum of ξ during time evolution. The factor $Q = (1 - \frac{m_e}{m_e^*})/(2r^2 \max \xi)$ is a nonmonotonous function of r, while its value at $r = r_\alpha^{\rm q}$ presented in Table I decreases monotonously.

IV. CONCLUSIONS

To summarize, we have computed the heterodyne conductivities in a 2DEG subject to a time-oscillating magnetic field, both for the classical and quantum cases. We schematically illustrate our findings in Fig. 5 and discuss several problems we would like to investigate in the future. (i) The many-particle state is realized by filling the states with $N_e = \nu N_\Phi$ electrons, as indicated in Fig. 5(b). Since the system is heated by the external driving, it is likely to have states with mixed Landau orbitals n. The effect of Coulomb interaction may lead to interesting effects. The electron wave functions overlap simultaneously around $x = 0$ during the time evolution [Fig. 5(c)]. This causes the interaction between states with different k_y to be enhanced and long-ranged. If the system can be stabilized and cooled, ordering such as ferromagnetism, a Wigner crystal, and even an analog of the fractional QHE state might be induced. However, it is also likely that the accumulation of a macroscopic number of electrons will make the system unstable and even destroy the sample along the line $x = 0$. (ii) Is the heterodyne Hall conductivity $\sigma_{yx}^{0,1}$ a topological quantity? Similar to the traditional IQHE [1,17], the current expression (27) is proportional to ν and is thus quantized. The renormalized coefficient $\frac{e^2}{h}Q$ is fixed as long as the magnetic field B is changed simultaneously with the frequency Ω with respect to the quantization condition $r = r_\alpha^{\rm q}$. To answer this question, an edge calculation and an extension of the TKNN formula [2] is important, which may reveal a bulk-boundary correspondence [26] in heterodynes. (iii) Physical realization is an important problem. The driving field (13) can be realized by placing two antiparallel wires with currents oscillating as $\pm I \cos(\Omega t)$. The 2DEG is to be placed between the wires. This setup may be realized using THz plasmonics, with which it is already possible to generate magnetic fields with strength above 1 T oscillating in the terahertz domain [27,28]. This is the strength and frequency necessary to realize the quantization condition and to be in the quantum limit, i.e., small ν.

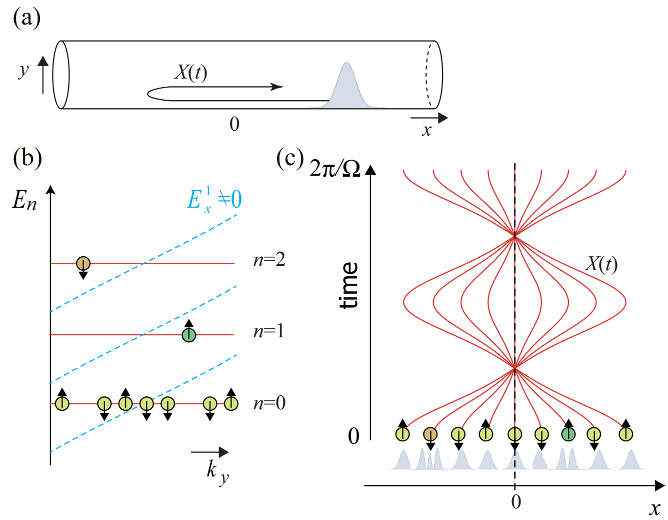

FIG. 5. (a) Schematic representation of the particle's dynamics. The wave function is a plane wave with momentum k_y along the y direction (represented as a compactified dimension, assuming L_y is finite) and a localized wave packet oscillating along the x direction. (b) When the Landau quantization condition $r = r_\alpha^{\rm q}$ is met, the Floquet quasienergy becomes flat (linearly tilted) in the absence (presence) of $E_x(t) = E_x^1 \cos(\Omega t)$. The many-particle state is achieved by filling the states with electrons with a spin, denoted as circles with an arrow, respecting the Pauli principle. (c) The motion of the wave-packet center for the many-particle state in (b). The initial position $X(0)$ depends on k_y; wave packets with different k_y evolve independently and oscillate around $x = 0$ according to (18).

ACKNOWLEDGMENTS

We thank Masaaki Nakamura and Yu Mukai for illuminating discussions. T.O. acknowledges Stefan Kaiser, Thomas Weiss, Koichiro Tanaka, and Andre Eckardt for fruitful discussions. This work is partially supported by KAKENHI (Grant No. 23740260) and the ImPact project (No. 2015-PM12-05-01) from JST.

[1] K. V. Klitzing, G. Dorda, and M. Pepper, Phys. Rev. Lett. **45**, 494 (1980).
[2] D. J. Thouless, M. Kohmoto, M. P. Nightingale, and M. den Nijs, Phys. Rev. Lett. **49**, 405 (1982).
[3] A. Maznev, K. Nelson, and J. Rogers, Opt. Lett. **23**, 1319 (1998).
[4] R. W. P. Drever, J. L. Hall, F. V. Kowalski, J. Hough, G. M. Ford, A. J. Munley, and H. Ward, Appl. Phys. B **31**, 97 (1983).
[5] W. Lenth, Opt. Lett. **8**, 575 (1983).
[6] R. G. Mani, J. H. Smet, K. von Klitzing, V. Narayanamurti, W. B. Johnson, and V. Umansky, Nature (London) **420**, 646 (2002).
[7] I. A. Dmitriev, A. D. Mirlin, D. G. Polyakov, and M. A. Zudov, Rev. Mod. Phys. **84**, 1709 (2012).
[8] T. Oka and H. Aoki, Phys. Rev. B **79**, 081406 (2009).
[9] T. Kitagawa, T. Oka, A. Brataas, L. Fu, and E. Demler, Phys. Rev. B **84**, 235108 (2011).

[10] N. H. Lindner, G. Refael, and V. Galitski, Nat. Phys. **7**, 490 (2011).
[11] M. S. Rudner, N. H. Lindner, E. Berg, and M. Levin, Phys. Rev. X **3**, 031005 (2013).
[12] F. D. M. Haldane, Phys. Rev. Lett. **61**, 2015 (1988).
[13] M. C. Rechtsman, J. M. Zeuner, Y. Plotnik, Y. Lumer, D. Podolsky, F. Dreisow, S. Nolte, M. Segev, and A. Szameit, Nature (London) **496**, 196 (2013).
[14] G. Jotzu, M. Messer, R. Desbuquois, M. Lebrat, T. Uehlinger, D. Greif, and T. Esslinger, Nature (London) **515**, 237 (2014).
[15] J. E. Müller, Phys. Rev. Lett. **68**, 385 (1992).
[16] D. Irawan, S. Viridi, S. N. Khotimah, F. D. E. Latief, and Novitrian, AIP Conf. Proc. **1656**, 060009 (2015).
[17] S. M. Girvin, in *Topological Aspects of Low Dimensional Systems*, edited by A. Comtet, T. Jolicoeur, S. Ouvry, and F. David (Springer-Verlag, Berlin and Les Editions de Physique, Les Ulis, 2000), p. 53.
[18] H. Sambe, Phys. Rev. A **7**, 2203 (1973).
[19] J. H. Shirley, Phys. Rev. **138**, B979 (1965).
[20] M. Grifoni and P. Hänggi, Phys. Rep. **304**, 229 (1998).
[21] A. G. Fainshtein, N. L. Manakov, and L. P. Rapoport, J. Phys. B **11**, 2561 (1978).
[22] K. Husimi, Prog. Theor. Phys. **9**, 381 (1953).
[23] L. S. Brown, Phys. Rev. Lett. **66**, 527 (1991).
[24] S. Blanes, F. Casas, J. Oteo, and J. Ros, Phys. Rep. **470**, 151 (2009).
[25] E. S. Mananga and T. Charpentier, J. Chem. Phys. **135**, 044109 (2011).
[26] Y. Hatsugai, Phys. Rev. Lett. **71**, 3697 (1993).
[27] T. J. Yen, W. J. Padilla, N. Fang, D. C. Vier, D. R. Smith, J. B. Pendry, D. N. Basov, and X. Zhang, Science **303**, 1494 (2004).
[28] Y. Mukai, H. Hirori, T. Yamamoto, H. Kageyama, and K. Tanaka, New J. Phys. **18**, 013045 (2016).